AAS 09-380

GLOBAL PERFORMANCE CHARACTERIZATION OF THE THREE BURN TRANS-EARTH INJECTION MANEUVER SEQUENCE OVER THE LUNAR NODAL CYCLE

Jacob Williams,* Elizabeth C. Davis,† David E. Lee,‡
Gerald L. Condon,§ Timothy F. Dawn¶ and Min Qu‖

The Orion spacecraft will be required to perform a three-burn trans-Earth injection (TEI) maneuver sequence to return to Earth from low lunar orbit (LLO). The origin of this approach lies in the Constellation Program requirements for access to any lunar landing site location combined with anytime lunar departure (which could require up to a 90° plane change). This paper documents the development of optimized trajectory databases used to rapidly model the performance requirements of the TEI three-burn sequence for an extremely large number of mission cases. It also discusses performance results for lunar departures covering a complete 18.6 year lunar nodal cycle as well as general characteristics of the optimized three-burn TEI sequence.

INTRODUCTION

Use of a three-burn maneuver sequence to transfer from a circular orbit to an escape hyperbola has been studied since 1959 when it was first proposed as a method to save propellant over one and two-burn escape sequences.[1] During the Apollo lunar program, this approach was investigated as a possible maneuver sequence to use for trans-Earth injection (TEI),[2–10] and the reverse problem (transfer from a hyperbolic to a circular orbit) was also studied for lunar orbit insertion (LOI) applications.[11,12] The three-burn escape maneuver sequence was also studied for applications to interplanetary missions.[13] These early studies provided valuable insight into the problem, but made many simplifying assumptions in order to obtain performance data in a reasonable amount of time. The most common assumption was to ignore the influence of the Earth's gravity during the maneuver sequence. Ultimately, the three-burn sequence was not employed during the Apollo program.

The three-burn TEI problem received renewed interest in 2004 with the inception of the NASA Constellation program to return humans to the Moon.[14–17] The current Constellation lunar architecture requires the Orion vehicle to provide access to the entire lunar surface with an anytime abort return capability. This requirement means that the vehicle must be capable of executing up to a 90° plane change to transfer from low lunar orbit (LLO) to the hyperbolic Earth return trajectory. In order to make this possible without a prohibitively large propellant cost, a three-burn TEI maneuver sequence is necessary. Initial Constellation work employed many of the same simplifications used in the Apollo-era studies, but as the Orion vehicle design matured, more refined estimates of flight

*ERC, Incorporated, Engineering and Science Contract Group, Houston, TX 77058
†Jacobs Technology, Engineering and Science Contract Group, Houston, TX 77058
‡EG/Aeroscience and Flight Mechanics Division, NASA Johnson Space Center, Houston, TX 77058
§EG/Aeroscience and Flight Mechanics Division, NASA Johnson Space Center, Houston, TX 77058
¶EG/Aeroscience and Flight Mechanics Division, NASA Johnson Space Center, Houston, TX 77058
‖Analytical Mechanics Associates, Hampton, VA 23666

performance became essential since they were being used to size the propellant tanks. Because the Constellation architecture is intended to be operational for a number of years, the entire range of possible Earth-Moon geometries must also be considered. A statistical approach to performance assessment was also desired, so that the vehicles are not over-designed to account for an insignificantly small percentage of worst-case mission scenarios.

At the NASA Johnson Space Center (JSC) Flight Mechanics and Trajectory Design Branch, the Copernicus trajectory design and optimization system[18] has been used extensively to study the TEI sequence for Constellation and Orion work*. Copernicus uses a multiple shooting parameter optimization approach with explicitly-integrated trajectory segments. It can be used to optimize end-to-end trajectories from low Earth orbit (LEO) to LLO, and from LLO to entry interface at the Earth, including complex environmental effects such as multi-body perturbations, high order Earth and Moon gravity models, and finite burn maneuvers.

The convergence time for fully optimized TEI trajectories represents a limiting factor on the number of cases which can practically be run. Given the range of mission variables (e.g., flight times, departure orbits, and entry constraints), it is not yet practical to generate fully optimized high-resolution end-to-end trajectories for billions of cases across an entire lunar nodal cycle. Therefore, a database approach was developed.[16] Strategic runs exploiting the high resolution trajectory optimization capability of Copernicus were used to construct databases of the performance costs for specific mission phases (such as the three-burn TEI sequence). These databases could then be used to quickly "look up" the performance of the various mission phases for specific cases, allowing the assessment of a huge number of mission permutations very quickly.

BACKGROUND AND FUNDAMENTALS

The Three-Burn Sequence

The two fundamental principles behind the three-burn TEI escape sequence are: (1) the direction of motion is most efficiently changed where the velocity is lowest, and (2) the energy level is most efficiently changed where the velocity is highest.[2] A schematic of the maneuver sequence is shown in Figure 1(a). The first maneuver (TEI-1) takes place in the initial circular orbit (currently baselined for Orion at 100 km altitude) and inserts the spacecraft into a large elliptical orbit about the Moon. The second maneuver (TEI-2) occurs near apoapsis of this intermediate orbit and performs most of the plane change. The third maneuver (TEI-3) takes place near periapsis of the second intermediate orbit and inserts the spacecraft onto the departure trajectory that returns to Earth. The TEI-1 and TEI-3 maneuvers are mostly coplanar, although they can each perform a small amount of plane change. The departure trajectory is hyperbolic with respect to the Moon, and elliptical with respect to the Earth. For Orion, the pre-TEI-3 periapsis altitude is limited to at least 100 km as a "fail safe" factor, to ensure that a failed TEI-3 will not result in a surface impact (since the optimal TEI-3 will generally occur just before periapsis of the second intermediate ellipse).

For Orion mission trade studies, the total flight time from TEI-1 to TEI-3 (Δt_{TEI}) has been limited to a maximum of 48 hours. With the current vehicle design, the most stressing missions will require a 48 hr TEI duration from TEI-1 to TEI-3, allowing the plane change maneuver to occur as far from the Moon as possible. For easier missions, where propellant margin is available, shorter flight times can be used. Operationally, other time constraints may be necessary to account for other factors, such as crew sleep cycles and navigation updates. When a large plane change is not

*Recent research involves generation of analytical initial guess trajectories to be used for optimizer initialization[19,20]

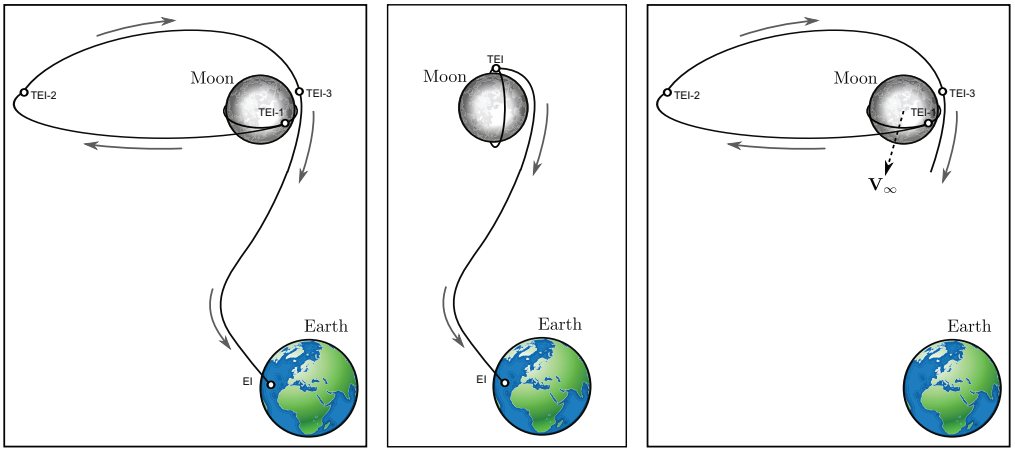

(a) Three Burn TEI to EI (b) Single Burn TEI to EI (c) Three Burn TEI V_∞ Target

Figure 1 Problem Setup. The full three-burn TEI to EI problem is subdivided into two separate problems: estimation of the $\mathbf{V}_\infty$ vector using a single-burn departure, and a three burn TEI sequence to target the $\mathbf{V}_\infty$ vector.

Table 1. Mission Cases

Mission Case	TEI-1 to TEI-3 (hrs)	TEI-3 to EI (hrs)	Earth Entry Constraints
Fast expedited A	24	89	h, γ
Fast expedited B	36	77	h, γ
Relaxed expedited	48	89	h, γ
Simplified Nominal	48	89	h, γ, Az
Entry Target Nominal	48	89 - 114	h, γ, Az, ϕ, λ

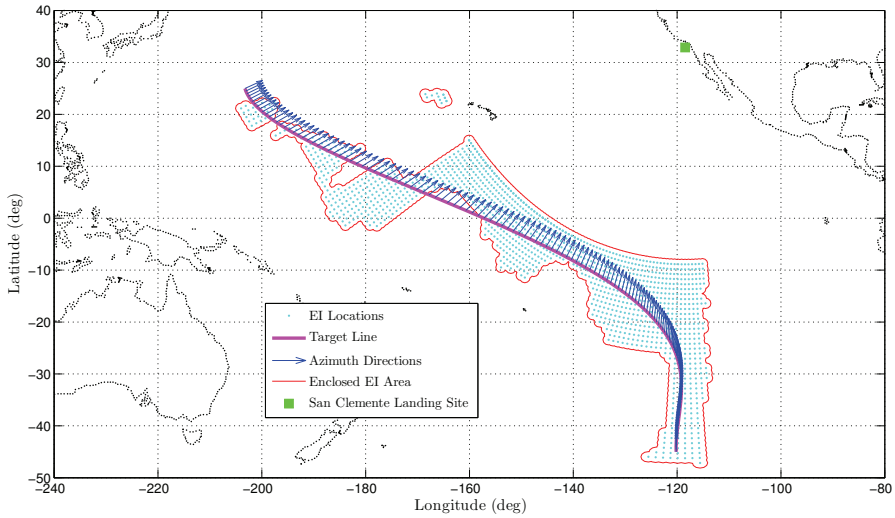

Figure 2 Entry Target Line Constraints. Sixth-order polynomials for longitude and azimuth as functions of latitude are used to impose entry constraints for landing off the coast of San Clemente Island. The target line is an approximation to the entry interface points.

required, a one-burn or two-burn sequence may be employed. These issues are not considered in this study.

Mission Cases

Five classes of missions, each defined by different flight times and Earth entry conditions, will be considered in this study. These mission cases (summarized in Table 1) are currently being used to determine the Orion vehicle tank size requirements. The Earth entry interface (EI) state at t_{EI} is parameterized as: altitude (h), latitude (ϕ), longitude (λ), velocity (v), azimuth (Az), and flight path angle (γ). For all cases, the EI state component h is specified to be 121.92 km and γ is specified to be -5.86°.

"Expedited return" missions are defined by EI constraints on altitude and flight path angle only, with no constraints on the location or direction of the entry point (latitude, longitude, or azimuth). They are designed for abort situations (e.g., vehicle or equipment failure, crew injury, etc.) where the vehicle must return to Earth quickly and/or compute maneuvers without contact with Earth, necessitating the use of simplified on-board non-optimal targeting methods. The fast expedited returns allow for a total transfer time (from TEI-1 to EI) of 113 hrs. There are two cases considered here (A and B), which are distinguished by the relative amount of time spent from TEI-1 to TEI-3, and from TEI-3 to EI. Relaxed expedited returns allow for a total transfer time of 137 hrs.

"Nominal" missions are more constrained at EI in order to target specific landing sites or regions.[21] For trade studies, the simplified nominal case targets a zero azimuth entry with a total transfer time of 137 hrs. This is an approximation of a worst-case targeted entry condition. The entry target nominal case enforces a specific relationship between latitude, longitude, and azimuth at EI in order to target a specific landing site. In this study, the entry target constraints are imposed by using two sixth-order polynomials expressing longitude and azimuth as functions of latitude, as shown in Figure 2. The polynomials are constructed from data corresponding to valid entry states for a U.S. coastal water landing near San Clemente Island.[21] The smooth polynomial constraints (rather than the discrete points of the entry map) are more suitable for the optimization process, and closely reflect the actual performance requirements. This case requires a variable flight time (from 137 to 162 hrs) to achieve the specified longitude.

Lunar Cycle

The 18.6 year lunar nodal cycle is the period in which the Moon's line of nodes (the intersection of the lunar orbit and ecliptic planes) completes one revolution. The Earth-Moon geometry is a critical driver for TEI performance and thus cannot be ignored when considering the performance cost of the three-burn sequence. The lunar nodal cycle used in this study is the period from January 1, 2018 to August 7, 2036. The full cycle allows a complete range of Earth-Moon-Sun geometries to be considered across the expected operational lifetime of the Orion vehicle.

GLOBAL PERFORMANCE DATABASES

Overview

The fundamental assumption of this study is that, for performance purposes, the three-burn TEI transfer problem can be divided into two sub-problems: (1) computation of a departure $\mathbf{V}_\infty$ vector at the Moon corresponding to the desired return trajectory, and (2) computation of a three-burn TEI sequence that achieves the desired $\mathbf{V}_\infty$ vector. Parameterized databases for each sub-problem can

be constructed and queried for any mission case to produce a TEI Δv value which agrees closely with the fully-optimized TEI to EI sequence. For this study, the databases are generated with the Copernicus trajectory optimization system, using the SNOPT optimizer.[22]

Table 2. Fixed Azimuth V_∞ Database Parameters.

Parameter	Range
Departure epoch	From 2018-01-01 to 2036-12-31 in 12 hr steps
Az	From -10° to 190° in 5° steps
Δt_R	From 65 hrs to 113 hrs in 12 hr steps

Table 3. Entry Target Nominal V_∞ Database Parameters.

Parameter	Range
Departure epoch	From 2018-01-01 to 2036-12-31 in 6 hr steps
Δt_R	2 cases (65-89 hrs, and 89-114 hrs)

$\mathbf{V}_\infty$ Vector Database

For a specified departure epoch (t_3), return flight time (Δt_R), and set of EI conditions (h, γ, and Az), the escape $\mathbf{V}_\infty$ vector can be estimated by optimizing a single-burn TEI departure from a circular polar lunar orbit (as shown in Figure 1(b)). The optimization variables for this problem are: longitude of the LLO ascending node (Ω_{LLO}), argument of latitude (u) of the maneuver, TEI Δv magnitude and direction, and the EI state parameters ϕ, λ, and v. In the problem setup, the entry state is integrated backwards in time (allowing the known EI parameters to be specified, rather than requiring them to be imposed as constraints), and the post-TEI maneuver state is integrated forwards in time. A state (position and velocity) equality constraint is imposed at the point one day after TEI to produce a continuous trajectory. The objective function to be minimized is the TEI Δv magnitude. The entry target case is slightly modified, since Δt_R and Az are also optimization variables, and polynomial constraints on ϕ, λ, and Az are imposed on the EI state.

The solution of this optimization problem produces two local minima, corresponding to two different Ω_{LLO} values separated by about 180°. These are referred to as the North and South solutions, since the spacecraft departs over either the lunar north or south pole. The vector average of these two $\mathbf{V}_\infty$ vectors at a given epoch provides an approximate vector which can be targeted from all orbits at that epoch. For the fully optimized TEI to EI problem, the $\mathbf{V}_\infty$ vector will vary slightly for different departure orbits, shown as an oval-shaped set of points in Figure 3(a), with the average vector being a point near the center of this oval. When joined together with the three-burn database, the epoch for the single-burn TEI maneuver becomes the epoch of TEI-3, and the $\mathbf{V}_\infty$ vector becomes the escape condition after TEI-3.

Two databases were generated: (1) a 3D database used for the nominal and expedited return cases with the following input parameters: TEI-3 departure epoch (t_3), transfer time from TEI-3 to EI (Δt_R), and Earth entry (EI) azimuth, and (2) a 1D database for the entry target nominal case, where the only input parameter is epoch. The entry target database is generated for specific 24 hr return time ranges (in this case, from 65 to 89 hrs, and from 89 to 114 hrs). Each database was generated by stepping through the epochs from 2018 to 2036, using the previous epoch as an initial guess, solving the optimization problem, and saving the average $\mathbf{V}_\infty$ vector for each case. The

run parameters for these database are given in Table 2 and Table 3. Example data from the fixed-azimuth database is shown in Figures 4(a) and 4(b). Each case can be solved in about 1 second using Copernicus. The fixed azimuth database produced a total of 2,276,484 cases (about 26 days of CPU time), and the entry target nominal database produced a total of 111,044 cases (about 31 hrs of CPU time).

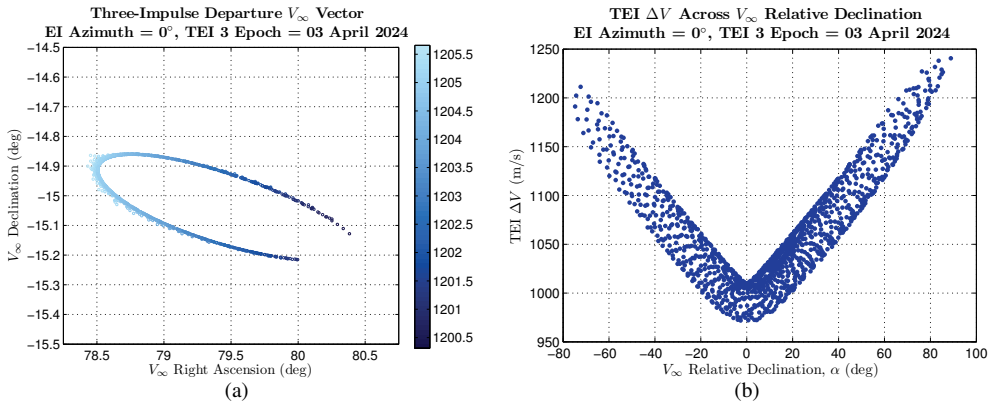

Figure 3 $\mathbf{V}_\infty$ vectors (colors indicate V_∞ magnitude in m/s) and TEI Δv for optimized three-burn departures to EI from a range of orbits for a simplified nominal mission case at a single epoch.

TEI Three-Burn Database with No Third-Body Perturbations

The starting point for investigating the three-burn TEI problem to target a $\mathbf{V}_\infty$ vector was to make the simplifying assumption that only the Moon's gravity affects the trajectory during the maneuver sequence. Under this assumption, the TEI Δv can be parameterized using only three reference parameters: (1) the magnitude of the $\mathbf{V}_\infty$ vector (V_∞), (2) the relative declination (α), the angle between the $\mathbf{V}_\infty$ vector and the LLO orbit plane, and (3) the time-of-flight from TEI-1 to TEI-3 (Δt_{TEI}). A database of this type was constructed with Copernicus using the parameter ranges given in Table 4 and was used in early Constellation and Orion studies.[16] Given these three parameters, the optimization variables for the three-burn TEI problem are: the argument of latitude (u) of TEI-1 in the LLO, the magnitudes and directions of each maneuver (TEI-1, TEI-2, and TEI-3), and the intermediate flight time from TEI-1 to TEI-2. A constraint is imposed that the post-TEI-3 escape hyperbola has the target $\mathbf{V}_\infty$ vector. The objective function to be minimized is the total TEI Δv magnitude ($\Delta v_1 + \Delta v_2 + \Delta v_3$). Given each input parameter permutation, a parking orbit and $\mathbf{V}_\infty$ vector are constructed, and a three-burn TEI sequence is optimized in Copernicus (as shown in Figure 1(c)) with only the Moon's gravity present in the force model. Representative results from

Table 4. 3D TEI Database Parameters

Parameter	Range
V_∞	From 700 to 1500 in 50 m/s steps
α	From 0° to 90° in 5° steps
Δt_{TEI}	From 1 day to 2 days in 0.25 day steps

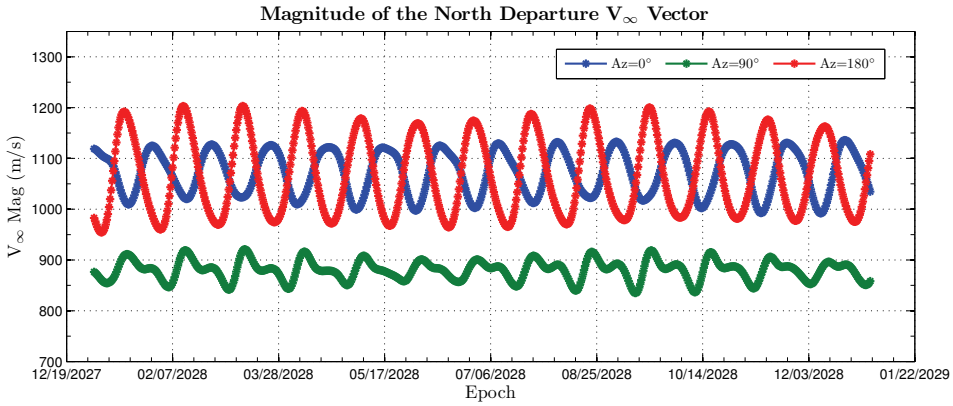

(a) Data from the 89 hour return time fixed-azimuth V_∞ database shows the variation of the V_∞ magnitude over a one-year period for different entry azimuths.

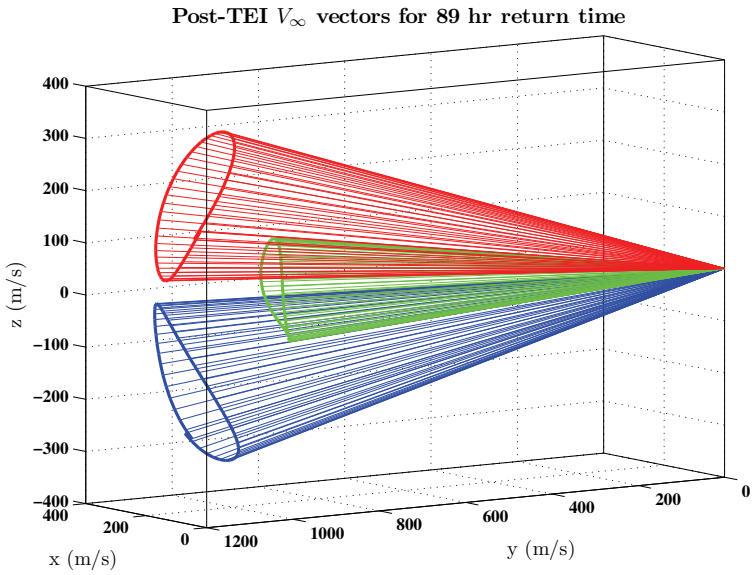

(b) V_∞ evolution for a one month period for the 89 hour return case (shown in a Moon-fixed reference frame).

Figure 4 Data from the fixed-azimuth V_∞ vector database for three entry azimuth values (0°, 90°, and 180°). Here, the vectors are expressed in a Moon-fixed frame.

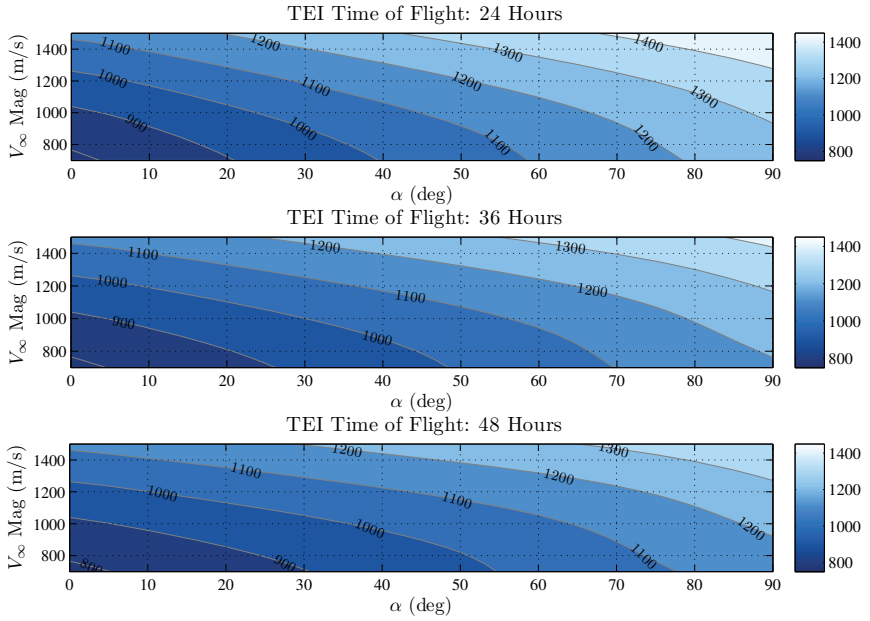

Figure 5. Data from the 3D TEI Database shows the TEI Δv (m/s) as functions of α, V_∞, and Δt_{TEI}.

this database are shown in Figure 5. Generally, the TEI Δv increases with increasing α, increasing V_∞, or decreasing Δt_{TEI}.

For a given mission case and departure epoch, the parameter that has the strongest influence on the TEI Δv is α, the relative declination angle between the initial orbit and the escape hyperbola. Figure 3(b) shows the dependence of TEI Δv on relative declination for the full TEI-1 to EI problem example given in the previous section. It is clear that, while there is a trend based on relative declination, other significant factors are also at play. The general effect of Earth gravity perturbations is to spread out the data points. The level of uncertainty from neglecting the third-body perturbation effect turned out to be up to $\pm$45 m/s for 48 hour TEI flight times, which was unacceptable for the purpose of sizing the Orion propellant tanks. However, the original three-parameter database captures the general trends of the data very well. It has a very high case density, and is amenable to interpolation via splines, so it is very responsive to the curvature and inflections of the data. For these reasons, it is still employed as part of the solution, as explained below.

Design of the TEI Three-Burn Database including Earth Perturbation Effects

Figure 6 shows the acceleration field due to Earth's gravity perturbation of an orbit about the Moon, expressed as a percentage of the lunar central-force acceleration. The scale is 10% per 5000 km (1 grid square) on the plot. The Earth is to the left of the plot on the x-axis, 384,400 km distant from the Moon. This field is symmetrical about the Earth-Moon axis. Unperturbed one-day (green) and two-day (red) orbits are shown for scale, with marks every three hours of travel. The perturbation acceleration, expressed as a fraction of the main-body acceleration, grows non-linearly with radius. For the two-day orbit, the most significant perturbation effects occur within $\pm$18 hours of apoapsis.

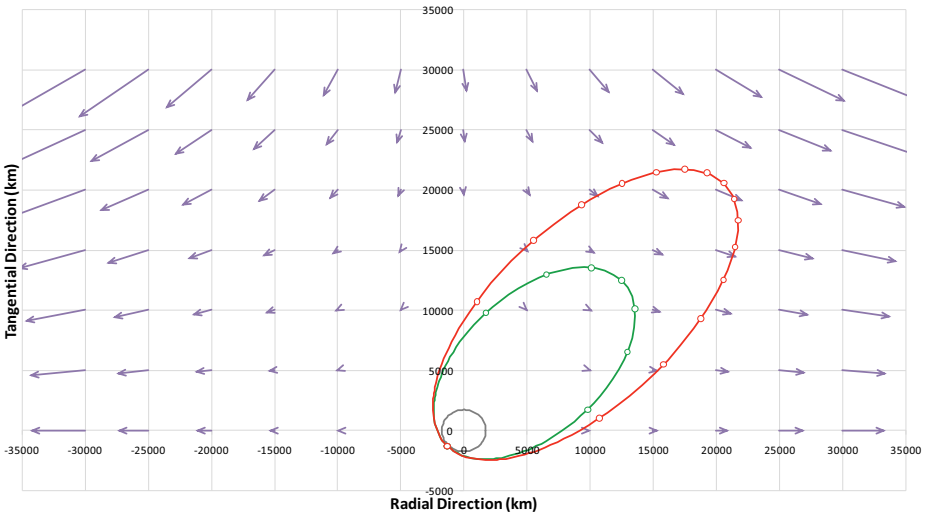

Figure 6 This plot shows accelerations due to Earth gravity perturbations of an orbit about the Moon, expressed as a percent of the central-force accelerations. The scale is 10% per 5000 km (1 grid square) on the plot. One day (green) and two day (red) orbits are shown for scale.

In designing the TEI three-burn sequence database that included Earth perturbation effects, the challenge was to identify the significant factors determining the perturbation effects of the Earth during the three-burn sequence and select the smallest possible parameter set to adequately represent these factors. Three vectors are sufficient to specify the orientation of the most important components of the problem:

$\mathbf{h_{LLO}}$ - The angular momentum vector of the initial LLO, together with the assumption of a circular orbit at 100 km altitude, defines the geometry of the initial orbit.

$\mathbf{R_E}$ - The vector from the Moon to the Earth at the midpoint epoch between TEI-1 and TEI-3 (t_M). This epoch is roughly the center of the period of the most pronounced perturbation accelerations (near apoapsis). As discussed above, the instantaneous direction of this vector determines the direction of the perturbation accelerations.

$\mathbf{V}_\infty$ - The V-infinity vector of the post-TEI-3 hyperbolic departure trajectory.

Note that each of these vectors occurs at a different epoch ($\mathbf{h_{LLO}}$ at t_1, $\mathbf{R_E}$ at t_M, and $\mathbf{V}_\infty$ at t_3), so they all must be referenced to a common non-rotating frame.

Fully specifying all of these vectors would require nine parameters, and fully defining their orientation would require six. However, specifying their orientation relative to one another is possible using only three angular parameters. See Figure 7 for an illustration of these angles. Note that these three angles begin our parameter list:

1. α - The relative declination of the $\mathbf{V}_\infty$ vector (i.e., the angle between the initial LLO plane and the $\mathbf{V}_\infty$ vector) with positive values when $\mathbf{V}_\infty$ falls on the same side of the plane as $\mathbf{h_{LLO}}$.

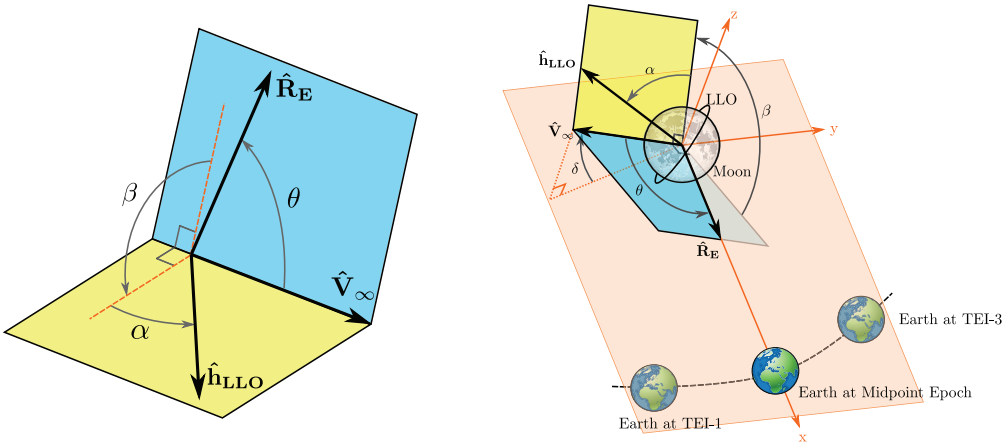

Figure 7 Three-Burn TEI Parameterization Geometry and the Moon-Earth Frozen Rotating Frame. The angles α, β, and θ define the relative orientation of the three vectors: $\mathbf{h_{LLO}}$, $\mathbf{R_E}$, and $\mathbf{V}_\infty$.

2. β - The angle between two planes: (1) the plane defined by $\mathbf{R_E}$ and the $\mathbf{V}_\infty$ vector, and (2) the plane defined by $\mathbf{h_{LLO}}$ and the $\mathbf{V}_\infty$ vector. The angle is measured in the right hand positive sense about the $\mathbf{V}_\infty$ vector from the first plane to the second.

3. θ - The angle between the $\mathbf{V}_\infty$ vector and $\mathbf{R_E}$.

The remaining parameters are:

4. Δt_{TEI} - Time of flight from TEI-1 to TEI-3. This determines the apoapsis distance of the trajectory, which will occur in the general vicinity of the midpoint time t_M. The perturbation effects due to the Earth are expected to be most pronounced near apoapsis, and the apoapsis distance will determine (along with the orientation of the orbit and the Earth-Moon distance) the magnitude of the perturbation accelerations encountered.

5. R_E - Distance from the Moon to the Earth at this midpoint time. This determines the magnitude of the perturbation accelerations and, to a lesser degree, the shape of the acceleration field.

6. V_∞ - Magnitude of the $\mathbf{V}_\infty$ vector from the Moon departure hyperbolic trajectory. This is a significant factor in determining the orientation of the maneuvers and intermediate orbits, and thus partially determines how the perturbations will affect the trajectory.

7. δ - the declination of the $\mathbf{V}_\infty$ vector with respect to the Earth-Moon orbit plane. As the Moon-Earth vector approaches, passes, and then moves away from the midpoint epoch, it will rotate in the Earth-Moon orbit plane. So this parameter captures information on how the Earth perturbation accelerations would vary over the period from TEI-1 to TEI-3.

Note that parameters 5 and 6 recapture the magnitude of two of the three defining vectors as scalars. So in effect, $\mathbf{R_E}$ and the $\mathbf{V}_\infty$ vector are completely defined in this model, if only in a

relative sense. Only the magnitude of $\mathbf{h_{LLO}}$ is unnecessary, since this orbit is uniformly specified to be a 100 km altitude circular orbit. This particular form of the parameter set has the advantage that it retains the parameters (V_∞, Δt_{TEI}, and α) of the simplified version of the TEI Δv database with no Earth perturbation effects.

Generation of the TEI Three-Burn Database with Earth Perturbations

Table 5. 7D TEI Database Parameters

Parameter	Range
V_∞	From 800 to 1450 in 108.33 m/s steps
R_E	From 356445 to 406706 in 12565.25 km steps
Δt_{TEI}	From 1 to 2 in 0.5 day steps
δ	0°
θ	From 35° to 105° in 14° steps
α	From -90° to 90° in 5° steps and ±1°, ±2°, ±88°, ±89°
β	From 0° to 360° in 10° steps

The parameters for the 7D database are given in Table 5. First, epochs were selected which represent the different distances (maximum, minimum, and three intermediate distances) from the Moon to the Earth. Values for θ and V_∞ were selected to correspond to expected ranges of these values for the missions being considered here. The parameters α and β have the full range of possible values. Three flight times, and one declination case was run. For this study, only 6 of the parameters are used, since only one δ case was generated in the database. The maximum value of δ is not large (roughly within $\pm 11^\circ$ for the Moon to Earth transit times considered here), and TEI Δv sensitivity to this parameter was found to be on the order of only 3 m/s. Future database refinement may include additional points for this parameter.

To generate the database, each permutation of the database parameter set must be used to construct and solve a three-burn optimization problem. This requires the generation of the LLO angular momentum vector ($\mathbf{h_{LLO}}$) and $\mathbf{V}_\infty$ vector for each case. The $\mathbf{V}_\infty$ vectors generated would not, in general, result in trajectories which would return to the Earth. Instead, these vectors are intended to bracket all of the real-world cases for which we might need to reference the data. The real-world $\mathbf{V}_\infty$ vectors, which would produce trajectories returning to the full range of desired entry conditions, should be encompassed by the values of the cases run.

Since each of the three parameter vectors is defined at a different epoch, they must all be represented in the same non-rotating frame. Although technically any non-rotating reference frame could be used for the construction of these vectors, it is convenient to use the Moon-Earth Frozen Rotating (MEFR) frame (frozen indicating that it is a "snapshot" in time of a rotating frame, to make a non-rotating one). Using this frame makes construction of some of the vectors much simpler. The MEFR frame is a Moon-centered non-rotating frame defined at the midpoint time of the three-burn sequence ($t_M = (t_1 + t_3)/2$), as shown in Figure 7. The x-axis points in the Earth direction, the z-axis is along the angular momentum direction of the Earth-Moon system, and the y-axis completes the right-handed set. In this frame, the Earth's position with respect to the Moon is not fixed. Note that, in general, $t_M \neq t_2$ (i.e., the second maneuver does not occur exactly at the midpoint time). Based on the definition of the MEFR frame, the Moon-Earth vector is known for a given epoch to be:

$$\mathbf{R_E} = R_E(t_M) \begin{bmatrix} 1 & 0 & 0 \end{bmatrix}^T \tag{1}$$

where $R_E(t_M)$ is the magnitude of the Earth-Moon distance at the midpoint time, obtained from the ephemeris (in this case, DE 421). The $\mathbf{V}_\infty$ vector right ascension α_∞ is computed from θ and δ (using Napier's rules for right spherical triangles) by:

$$\alpha_\infty = \arccos(\cos(\theta)/\cos(\delta)) \tag{2}$$

where right ascension and declination are defined with respect to the MEFR frame. Then, the $\mathbf{V}_\infty$ vector (in Cartesian coordinates) is computed via:

$$\mathbf{V}_\infty = V_\infty \left[\begin{array}{ccc} \cos(\alpha_\infty)\cos(\delta) & \sin(\alpha_\infty)\cos(\delta) & \sin(\delta) \end{array} \right]^T \tag{3}$$

With this information, the following unit vectors can be generated:

$$\widehat{\mathbf{U}}_\mathbf{3} = \mathbf{V}_\infty / V_\infty \tag{4}$$

$$\widehat{\mathbf{U}}_\mathbf{2} = (\mathbf{V}_\infty \times \mathbf{R_E}) / \|\mathbf{V}_\infty \times \mathbf{R_E}\| \tag{5}$$

$$\widehat{\mathbf{U}}_\mathbf{1} = \widehat{\mathbf{U}}_\mathbf{2} \times \widehat{\mathbf{U}}_\mathbf{3} \tag{6}$$

These will serve as a framework for construction of the LLO angular momentum vector, which can be done as follows:

$$\widehat{\mathbf{h}}_\mathbf{LLO} = \cos(\alpha)\cos(\beta)\widehat{\mathbf{U}}_\mathbf{1} + \cos(\alpha)\sin(\beta)\widehat{\mathbf{U}}_\mathbf{2} + \sin(\alpha)\widehat{\mathbf{U}}_\mathbf{3} \tag{7}$$

The angular momentum vector can then be converted into the LLO orbit inclination, i_{LLO}, and longitude of the ascending node, Ω_{LLO}.

This completes the inputs to the TEI optimization problem for generation of the TEI Earth perturbation database. This problem is identical to the no-perturbation TEI problem, except that the Earth's gravity is included in the force model (as shown in Figure 1(c)). All the permutations of the input parameters resulted in 1,048,950 cases. Each case took an average of 7 seconds to optimize in Copernicus. The entire database required about 85 days of CPU time to complete.

The database was generated by running Copernicus in a series of 7 nested loops (one for each of the parameters). The order of the loops was: Δt_{TEI}, V_∞, R_E, θ, δ, β, α. In each loop, the previous solution is used as the initial guess for the next solution. The α loop is divided into two sub-loops (from -90° to 0°, and from 90° to 10°). This aids in convergence, since stepping from high to low relative declination magnitude was found to provide better initial guesses than going from low to high. Furthermore, the existence of multiple solution families in the three-burn problem in the presence of Earth perturbations must be accounted for. In the region of high values of α (i.e., high relative declination), there can exist two locally optimal solutions, either of which could be the global minimum. Generally, one has a plane change at TEI-2 that is less than 90°, and the other has a greater than 90° plane change. Both of these cases are solved for, and the one with the lowest TEI Δv is selected for the database.

Each point in the 7D database is then post processed to compute the Δv difference (due to the Earth gravity perturbations) from the corresponding point in the lower-fidelity 3D database. This difference will be called the "Earth perturbation" magnitude (Δv_{EP}), and is computed by:

$$\Delta v_{EP} = \Delta v'_{TEI} - \Delta \widetilde{v}_{TEI} \tag{8}$$

Where $\Delta v'_{TEI}$ is the result from the 7D database, and $\Delta \widetilde{v}_{TEI}$ is the result from the 3D database (for the same value of V_∞, Δt_{TEI}, and α). With this, the 7D database becomes an Earth perturbation

database, returning the offset from the 3D database result. The reason that this strategy is employed (rather than using the 7D database directly to compute the Δv_{TEI}) is that the 3D database was generated at a finer resolution, uses spline interpolation, and better captures the curvatures and inflections of the data. The 7D database uses linear interpolation and has a coarser resolution. Combining the data in this way provides high resolution on the first-order trends, while the second-order Earth perturbation effects are adequately represented by the coarser data.

Figures 8-11 show TEI Δv and Earth perturbation (EP) results from the 7D database. Figures 8 and 10 show the minimum, mean, and maximum values as functions of each parameter. Figure 8 shows the sensitivity to TEI time of flight. As expected, while the maximum total TEI Δv decreases with longer TEI flight times, the maximum EP increases. For the two day flight time, the maximum EP is about $\pm$45 m/s. Figure 10 shows the EP variation for the other parameters (for the 48 hr TEI transfer time case). As expected, these indicate that the maximum EP also decreases with increasing Moon-Earth distance. Interestingly, the α plot shows that for the worst cases (α near $\pm 90^\circ$) the EP is always negative, meaning that the 3D database always overestimated the TEI Δv for these cases. For α near 0°, the EP is always positive, meaning that the 3D database always underestimated the TEI Δv for these cases. Figure 9 shows representative contours for a specific V_∞, R_E, and θ. Figure 11 shows the variation of the shape of the Earth perturbation contours as θ varies.

Querying the Databases

A schematic of how the databases are used is shown in Figure 12. Multidimensional cubic B-spline interpolation[23] is used to query all the databases except the 7D TEI EP database (which uses linear interpolation). First, the $\mathbf{V}_\infty$ vector is looked up based on the TEI-3 epoch, the time-of-flight (or time-of-flight limits) from TEI-3 to EI, and the desired entry conditions (either the EI azimuth or the entry target polynomials). Once the $\mathbf{V}_\infty$ vector is known, it is used (along with the epoch, initial orbit, and TEI flight time) to compute the parameter inputs to the TEI databases. The angles α, β, and θ can be computed by*:

$$\alpha = atan2\left[(\mathbf{h_{LLO}} \cdot \mathbf{V}_\infty), \|\mathbf{h_{LLO}} \times \mathbf{V}_\infty\|\right] \quad (9)$$

$$\beta = atan2\left[(\mathbf{R_E} \times \mathbf{V}_\infty) \times (\mathbf{h_{LLO}} \times \mathbf{V}_\infty) \cdot \mathbf{V}_\infty / V_\infty, (\mathbf{R_E} \times \mathbf{V}_\infty) \cdot (\mathbf{h_{LLO}} \times \mathbf{V}_\infty)\right] \quad (10)$$

$$\theta = atan2\left[\|\mathbf{R_E} \times \mathbf{V}_\infty\|, (\mathbf{R_E} \cdot \mathbf{V}_\infty)\right] \quad (11)$$

The 3D and 7D TEI databases are used together to compute the TEI Δv. The 3D database produces a solution $\Delta\widetilde{v}_{TEI}$ (without Earth perturbations), and the 7D database produces the Earth perturbation value Δv_{EP}. The two are used to compute the three-burn Δv_{TEI} by:

$$\Delta v_{TEI} = \Delta\widetilde{v}_{TEI} + \Delta v_{EP} \quad (12)$$

For the expedited return missions, the EI azimuth is a free parameter. The databases are queried by a global search routine to find the entry azimuth corresponding to the lowest TEI Δv. The fixed-azimuth $\mathbf{V}_\infty$ database is used in this case. In general, there can be two local minima for this problem, which have two different departure $\mathbf{V}_\infty$ vectors at the Moon. These two solutions correlate with the two TEI sequence solution families.

*The $atan2$ functions use the Fortran convention of a sine, cosine (or Y value, X value) order of inputs.

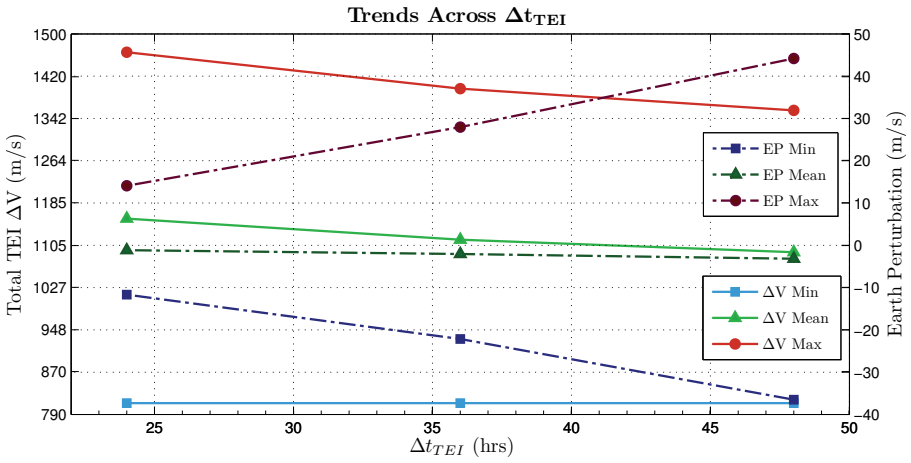

Figure 8 Plot showing how the Earth Perturbation changes for different values of Δt_{TEI}. As expected, the maximum Earth perturbations occur for longer flight times.

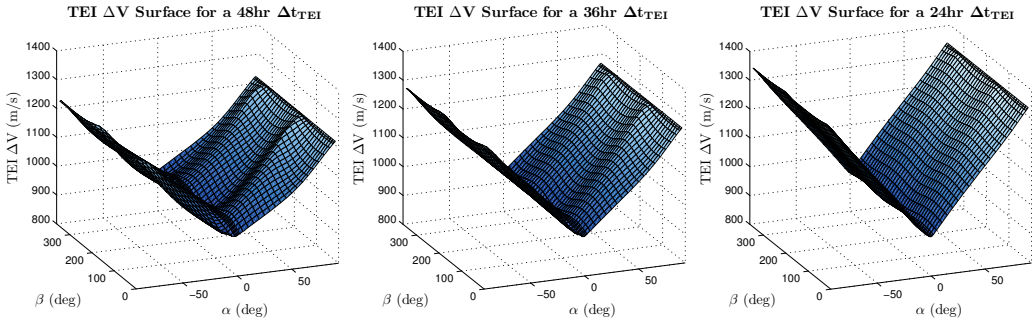

(a) Total TEI Δv

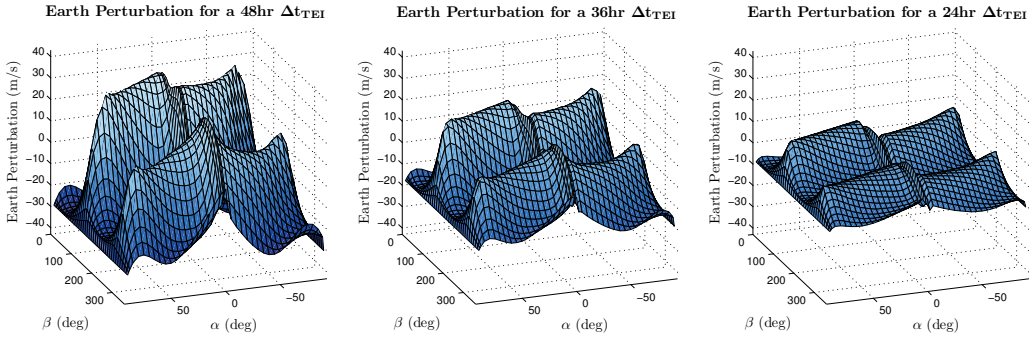

(b) Earth Perturbation Δv_{EP}

Figure 9 TEI Δv(a) and EP Surfaces showing the effect of TEI flight time across the parameters α and β. All data shown is for the case where V_∞ = 1125 m/s, R_E = 381576 km, and θ = 77°

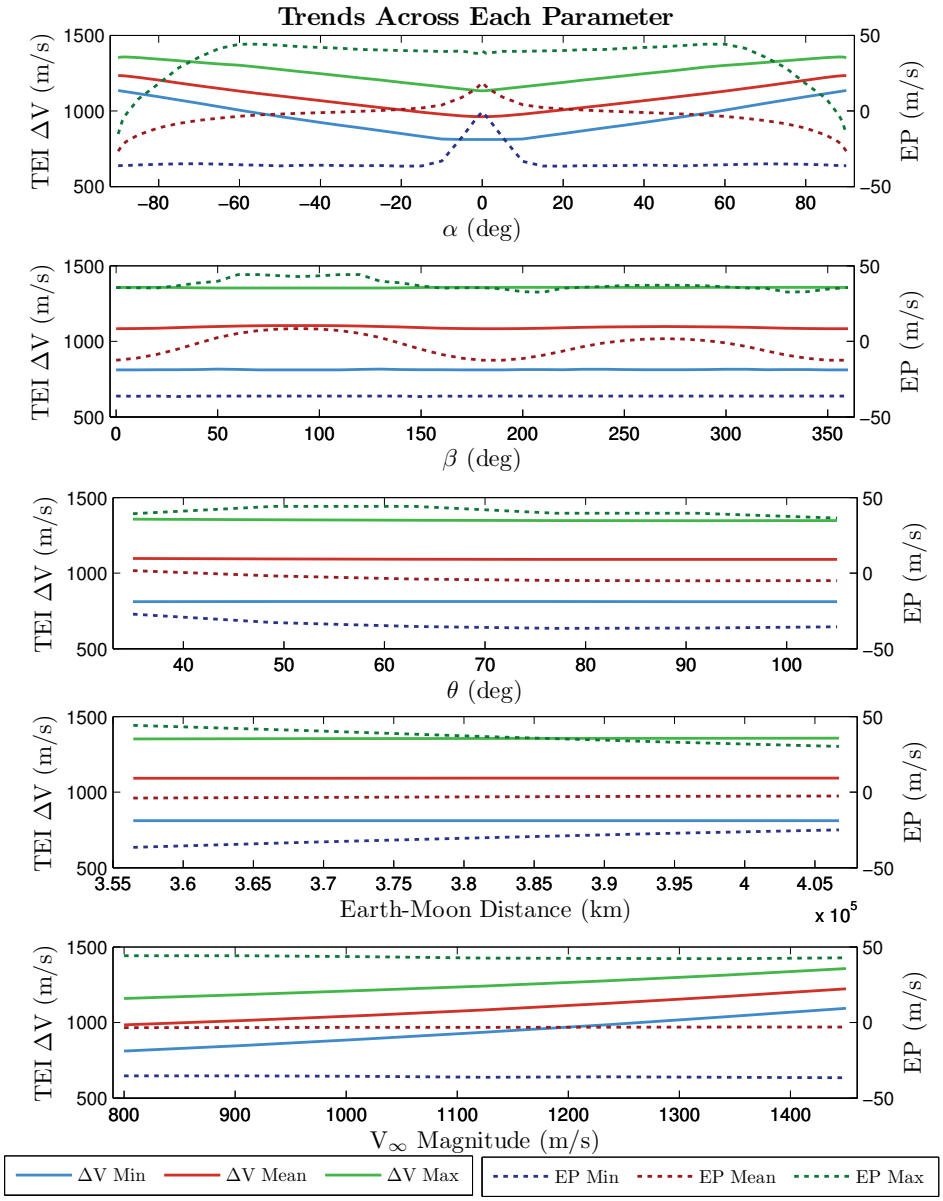

Figure 10 Figure shows the maximum, mean, and minimum trends for total TEI Δv and Earth Perturbation Δv_{EP} for the specified database parameter. These values were calculated across all other parameters. Results shown are for the 48 hr time of flight case.

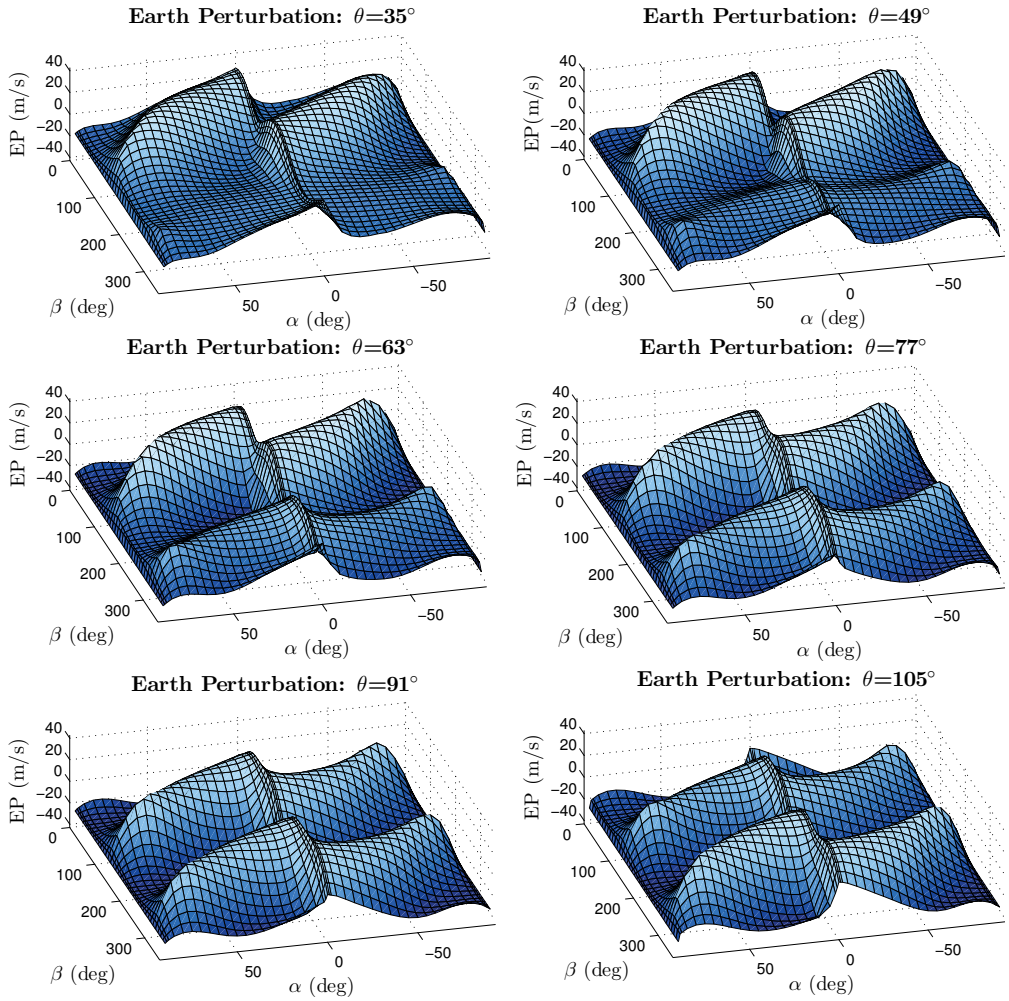

Figure 11 Plots showing how the Earth Perturbation changes for different values of θ. All plots shown are for the case where V_∞ = 1125 m/s, R_E = 368576 km, and Δt_{TEI} = 48 hrs.

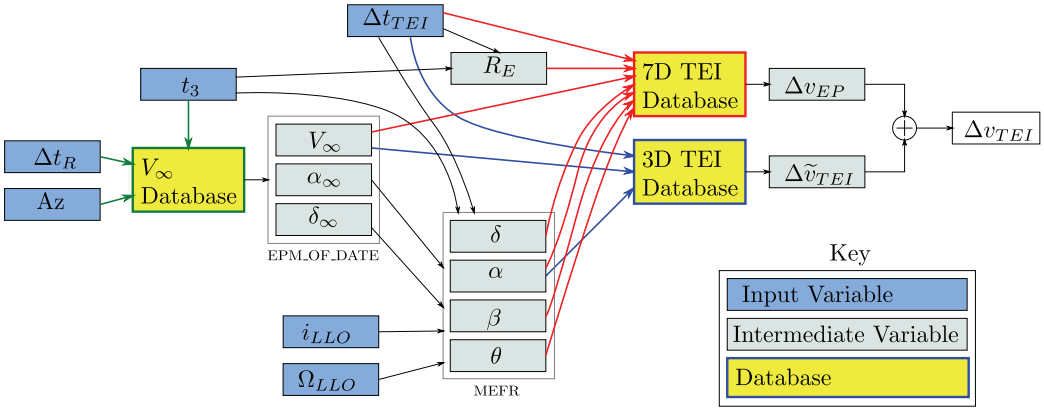

Figure 12 TEI Database Methodology. This diagram shows how the 6 inputs (blue boxes) are used to compute inputs to the 3 databases (yellow boxes) to produce the TEI Δv result. The computation requires several intermediate variables to be computed.

RESULTS AND CONCLUSIONS

The database querying process is very fast (about 5000 queries per second on a desktop PC), allowing a very large number of mission cases to be quickly assessed. A scan was conducted for each mission case listed in Table 1 of all retrograde departure orbits at 5° resolution in inclination, 10° resolution in longitude of the ascending node, and 6 hr resolution in time for the 2018-2036 lunar cycle. Figure 13 shows a snapshot of this data at a single epoch. Figure 14 shows the three-burn TEI Δv corresponding to the best and worst case departure orbits for each of the mission cases for the entire lunar cycle. Table 6 shows a summary of the worst-case epochs over this period for each mission case. A comparison is given with the database results and fully-optimized results from Copernicus. For each of these cases, the database is within 0.2% of the optimized result.

The TEI performance database is a powerful tool for mission trades and vehicle performance studies and has been used extensively in the Orion project. It allows the determination of the maximum TEI Δv required to complete a given mission type over the entire lunar cycle and provides a statistical view of mission coverage for lower vehicle capability values. It enables a highly-detailed overview of the three-burn TEI performance which would not otherwise be available and is being used for both vehicle and mission design.

Table 6. Worst Cases: Comparison of Database with Optimized Results from Copernicus

	Fast Expedited A	Fast Expedited B	Relaxed Expedited	Simplified Nominal	Entry Target Nominal
LLO INC (deg)	95	95	95	100	105
LLO LAN (deg)	0	160	180	190	200
TEI-1 Epoch (TDB)	11/7/2033 6:00	1/25/2028 12:00	3/12/2029 6:00	4/5/2024 0:00	4/25/2025 6:00
Database TEI Δv (m/s)	1264.96	1233.01	1156.39	1239.84	1236.83
Copernicus TEI Δv (m/s)	1263.66	1231.67	1155.38	1238.83	1238.99
Error (m/s)	-1.30	-1.35	-1.02	-1.00	2.16
% Error	0.10	0.11	0.09	0.08	0.17

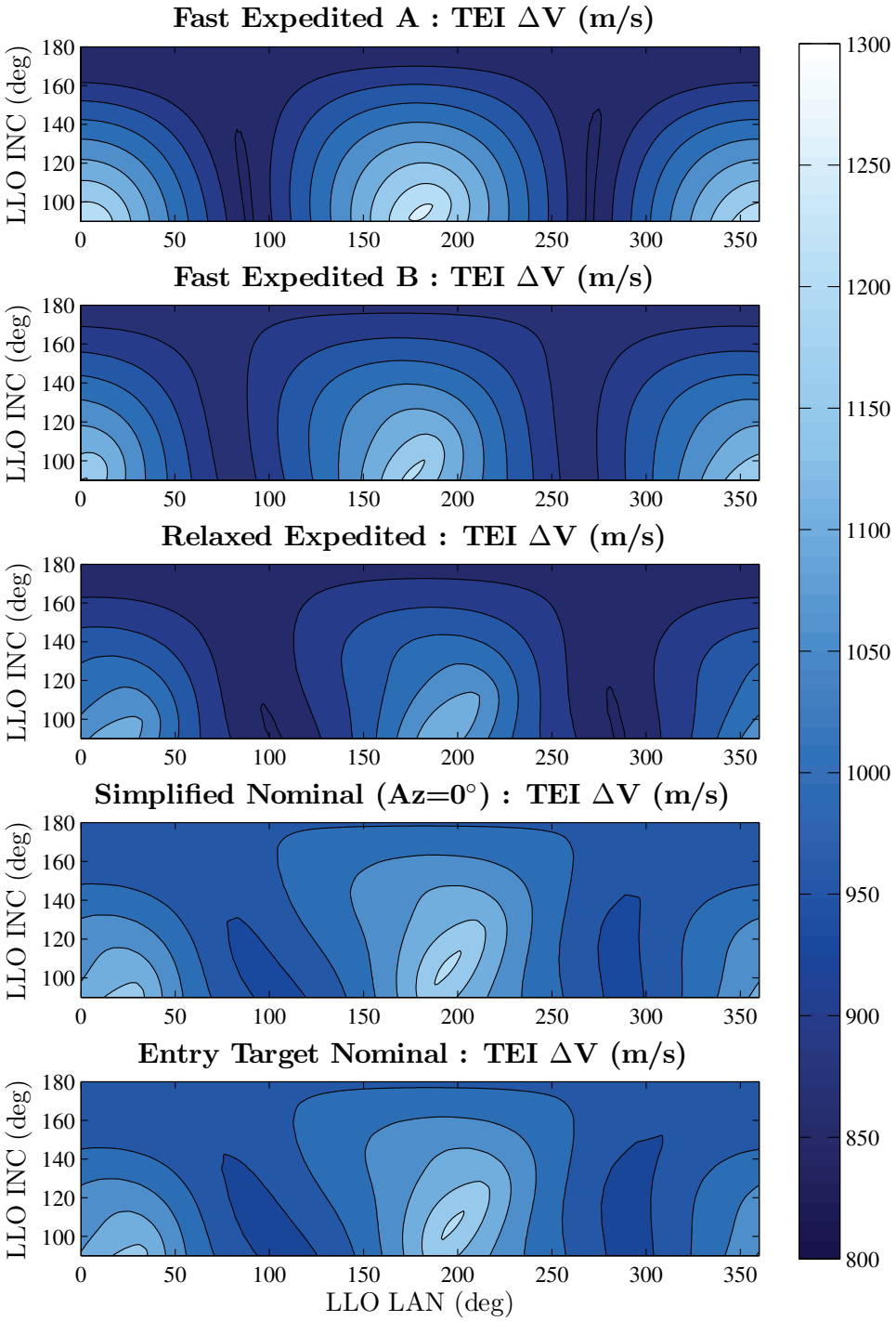

Figure 13 TEI Δv contour plots showing retrograde lunar orbit departures for each mission case, where TEI-1 occurs on January 1, 2018.

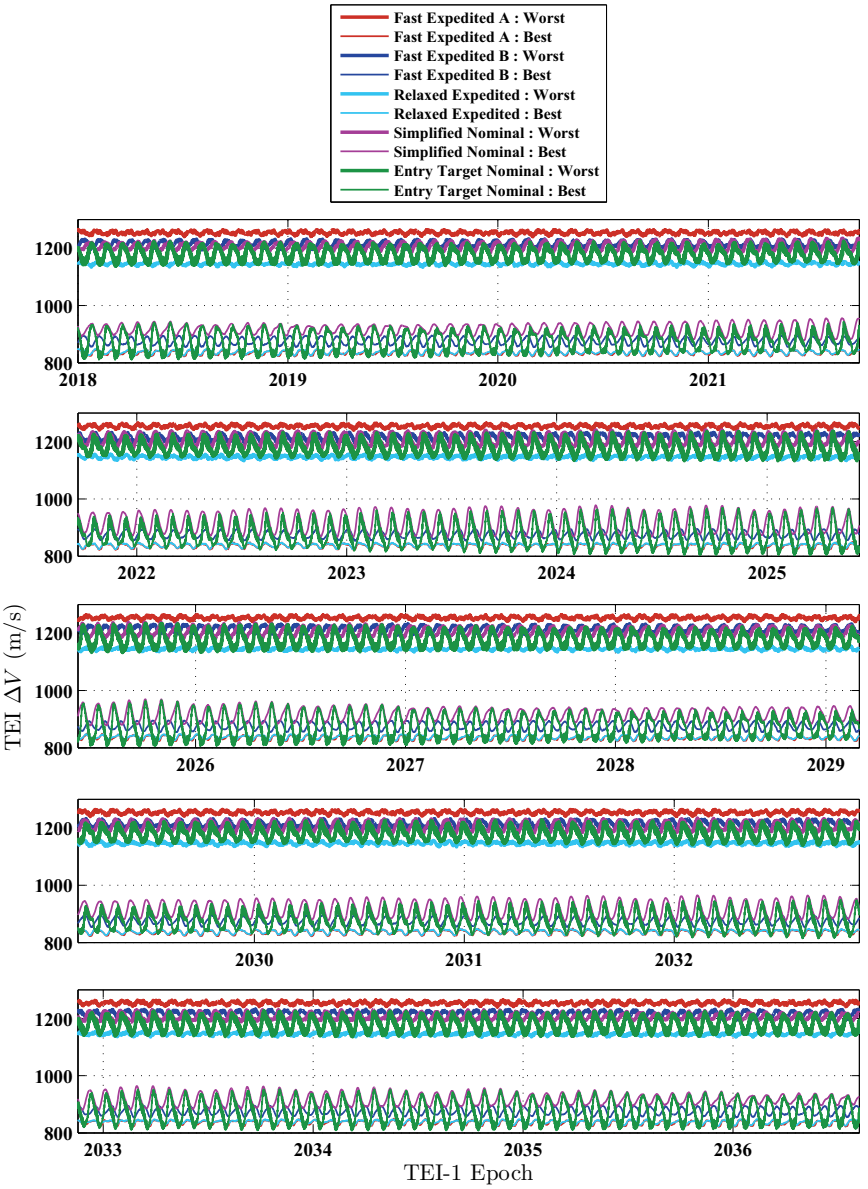

Figure 14 Performance Results Over the Lunar Cycle. This plot shows the best (lowest Δv_{TEI}) and worst (highest Δv_{TEI}) departure orbits at each epoch for each mission case.

ACKNOWLEDGMENT

This work was funded by the NASA Constellation and Orion projects. The authors would like to acknowledge Ryan Whitley, who developed the entry interface target line polynomials. Special thanks also to Juan Senent, Shaun Stewart, Andy Scott, Jeremy Carnahan, and Mike Frostad.

REFERENCES

[1] T. N. Edelbaum, "Some Extensions of the Hohmann Transfer Maneuver," *ARS Journal*, Vol. 29, 1959, pp. 864–865.

[2] E. D. Webb, "A Preliminary Analysis of a Three-Impulse Technique for Transearth Injection From Highly Inclined Orbits," Contractor Report 92164, NASA, May 1966.

[3] E. D. Webb, "Three Impulse-Transfer From Lunar Orbits," *Space Flight Mechanics Specialist Symposium, AAS Science and Technology Series*, Vol. 11, July 1966.

[4] T. N. Edelbaum, "How Many Impulses?," *Astronautics and Aeronautics*, Vol. 5, 1967, pp. 64–69.

[5] D. J. Jezewski and H. L. Rozendaal, "An Efficient Method for Calculating Optimal Free-Space N-Impulse Trajectories," *AIAA Journal*, Vol. 6, November 1968.

[6] R. J. Gerbracht, "Three-Impulse Transfers Between Elliptic and Hyperbolic Trajectories," Interoffice Correspondence 3421.1-6, TRW Systems, Jan 1968.

[7] P. A. Penzo, "A Pericenter Constrained Three-Impulse Optimization of Escape From a Circular Orbit," Interoffice Correspondence 3420.9-11, TRW Systems, January 1968.

[8] R. J. Gerbracht and P. A. Penzo, "Optimum Three-Impulse Transfer Between an Elliptic Orbit and a Non-Coplanar Escape Asymptote," *AAS/AIAA Astrodynamics Specialist Conference*, September 1968.

[9] P. A. Penzo, "A Three-Impulse Technique for the Real-Time Forward Iterator Program (RTFIP)," Interoffice Correspondence 5520.9-20, TRW Systems, September 1968.

[10] T. N. Edelbaum, "Optimal Nonplanar Escape from Circular Orbits," *AIAA Journal*, Vol. 9, December 1971.

[11] R. J. Gerbracht, "Restricted Three Impulse Transfer from a Hyperbolic Trajectory to a Circular Orbit," Interoffice Correspondence 3423.1-8, TRW Systems, September 1967.

[12] M. R. Kerr, "Parametric Analysis of Three-Impulse Transfer Between Hyperbolic Lunar Orbit and a Circular Lunar Parking Orbit," Technical Memorandum TM-70-2013-1, Bellcomm, Inc., March 1970.

[13] W. C. Bean, "Minimum Δ V, Three-Impulse Transfer Onto a Trans-Mars Asymptotic Velocity Vector," Technical Note D-5757, NASA, April 1970.

[14] "NASA's Exploration Systems Architecture Study Final Report," Technical Memorandum NASA-TM-2005-214062, NASA, November 2005.

[15] G. L. Condon, T. F. Dawn, R. S. Merriam, R. R. Sostaric, and C. H. Westhelle, "CEV Trajectory Design Considerations For Lunar Missions," *30th Annual AAS Guidance and Control Conference*, February 2007.

[16] G. Condon, J. Williams, and S. Stewart, "Trajectory Design and Performance Requirements for Human Lunar Missions Using the Mission Assessment Post-Processor (MAPP)," Technical Report FltDyn-CEV-08-162, NASA, February 2009.

[17] G. Condon and A. Scott, "Assessment of Orion Mission Capability as a Function of Driving Time and Geometry Related Factors," *AIAA Guidance, Navigation and Control Conference*, August 2008.

[18] C. Ocampo, "An Architecture for a Generalized Trajectory Design and Optimization System," *Proceedings of the International Conference on Libration Points and Missions*, June 2002. Girona, Spain.

[19] C. Ocampo and R. Saudemont, "Initial Trajectory Model for a Multi-Maneuver Moon to Earth Abort Sequence," *19th AAS/AIAA Spaceflight Mechanics Meeting*, February 2009.

[20] C. Ocampo, J. P. Munoz, and G. Condon, "Variational Equations for a Generalized Spacecraft Trajectory Model," *19th AAS/AIAA Spaceflight Mechanics Meeting*, February 2009.

[21] C. Lacefield *et al.*, "GN&C Design and Data Book Volume V - Entry, Descent and Landing," Document CEV-T-078005, Lockheed Martin Space Systems Company, 2009.

[22] P. E. Gill, W. Murray, and M. A. Saunders, "SNOPT: An SQP Algorithm for Large-Scale Constrained Optimization," *SIAM Journal on Optimization*, Vol. 12, No. 4, 2002.

[23] C. deBoor, "Package for Calculating with B-Splines," *SIAM Journal on Numerical Analysis*, Vol. 14, June 1977.